Available online at www.sciencedirect.com
SCIENCE DIRECT
ELSEVIER
International Journal of Machine Tools & Manufacture 46 (2006) 304–312
INTERNATIONAL JOURNAL OF MACHINE TOOLS & MANUFACTURE DESIGN, RESEARCH AND APPLICATION
www.elsevier.com/locate/ijmactool

An analysis of grinding power and surface roughness in external cylindrical grinding of hardened SCM440 steel using the response surface method

Jae-Seob Kwak*, Sung-Bo Sim, Yeong-Deug Jeong

School of Mechanical Engineering, Pukyong National University, San 100, Yongdang-Dong, Nam-Ku, Busan 608-739, South Korea

Received 19 January 2005; accepted 19 May 2005
Available online 6 July 2005

Abstract

The aim of this study was to analyze effectively the grinding power spent during the process and the surface roughness of the ground workpiece in the external cylindrical grinding of hardened SCM440 steel using the response surface method. A Hall effect sensor was used for measuring the grinding power of the spindle driving motor. The surface roughness was also measured and evaluated according to the change of the grinding conditions. Response surface models were developed to predict the grinding power and the surface roughness using the experimental results. From adding simply material removal rate to the contour plot of these mathematical models, it was seen that useful grinding conditions for industrial application could be easily determined.

Keywords: Grinding power; Surface roughness; External cylindrical grinding; Response surface method

1. Introduction

A lot of attempts have been made to describe more effectively and adequately the grinding process. This is dissimilar to other machining processes such as turning and milling, as the cutting edges of the grinding wheel don't have uniformity and act differently on the workpiece at each grinding. In spite of these attempts, typified by [1–3], describing the grinding action between the grinding wheel and the workpiece has not been made clear. So statistical models [4] and computer simulations [5] that could deal with the variety of the cutting edges were introduced. These complexities and difficulties of illustrating the grinding process also raise obstacles to the optimization of the grinding process and to the verification of the interrelationship between grinding parameters and outcomes of the process [6–7].

Malkin [8–9] investigated the process monitoring and studied various grinding phenomena such as cutting mechanisms, the specific energy and the interrelationship of the parameters during past decades. In his research, it was seen that the grinding process had very complex cutting mechanisms and also repeatability was difficult to obtain under the same grinding conditions. Shaji [10] reported a study on the Taguchi method for evaluating process parameters in surface grinding with graphite as lubricant. The effect of the grinding parameters (wheel speed, table speed, depth of cut and the dressing mode) on the surface finish and the grinding force was analyzed. Kwak [11] showed that the various grinding parameters affected the geometric error generated during the surface grinding by using the Taguchi method and also the geometric error could be predicted by means of the response surface method.

In this study, the response surface models are developed to predict the grinding power and the surface roughness in the external cylindrical grinding of the hardened SCM440 steel and also to help the selection of grinding conditions.

2. Literature review

2.1. Chip geometry of external cylindrical grinding

The cutting mechanism of the grinding process is very complex and not clear because the grinding wheel has many

* Tel.: +82 51 620 1622; fax: +82 51 620 1531.
E-mail address: jskwak5@pknu.ac.kr (J.-S. Kwak).

0890-6955/$ - see front matter © 2005 Elsevier Ltd. All rights reserved.
doi:10.1016/j.ijmachtools.2005.05.019

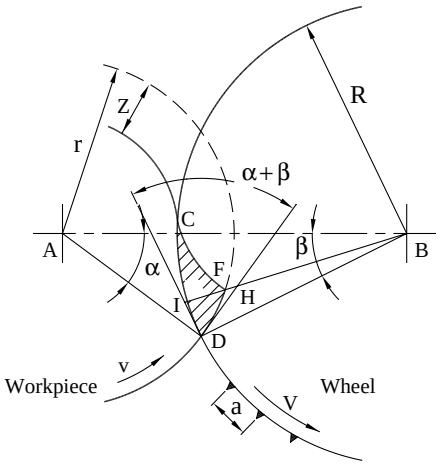

Fig. 1. Illustration of grinding depth and contact length.

irregular abrasives that are randomly distributed in the working area of the wheel circumference. Under several assumptions for convenience, the enlarged contact geometry in the external cylindrical grinding process can be simply illustrated as shown in Fig. 1.

From the chip geometry, it is seen that a cutting edge on the circumference of the grinding wheel contacts firstly a point C on the workpiece and then it moves along the arc CD (contact length) during the grinding. So the chip thickness in a viewpoint of the cutting edge increases gradually from C to I and peaks at point I. And then, the chip thickness decreases from I to D. The maximum chip thickness (g) in the cutting edge is about equal to the length HI and can be expressed as below.

$$g = HI = DH\sin(\alpha+\beta) = 2a\frac{v}{V}\sqrt{Z}\sqrt{\frac{d+D}{dD}} \tag{1}$$

Where d and D represent the workpiece diameter and the wheel diameter, respectively. Z is the depth of cut. The maximum chip thickness is mostly affected by an average distance (a) between the successive cutting edges at the grinding wheel and the speed ratio ($\frac{v}{V}$). The arc of the contact length (l_c) between the grinding wheel and the workpiece can also be represented by applying a small angle approximation.

$$l_c = 2\sqrt{Z}\sqrt{\frac{dD}{d+D}}\left(1+\frac{v}{V}\right) \tag{2}$$

Considering traverse speed f that is a traverse length per revolution in the workpiece, a tangential grinding force F_t and an energy P_o spent during grinding are as follows.

$$F_t = l_c Z^2 \frac{v}{V} f, \quad P_0 = F_t V \tag{3}$$

From Eq. (3), it is seen that the tangential grinding force (or energy) in the external cylindrical grinding directly concerns a selection of the grinding parameters.

2.2. Hall effect and grinding power measurement

Usually to measure the spent power of a machine during the process, the Hall effect sensor would be available in many types of industrial applications. The principle of the Hall effect sensor is based on the Hall effect, which was discovered by Dr Edwin Hall in 1879.

The current flowing through a cable from the driving motor of a grinding machine produces a magnetic field. If the cable passes into the Hall effect sensor, an induced voltage in the sensor is developed due to the Lorentz force. This voltage is known as the Hall voltage and the amount of the Hall voltage is proportional to the original current flowing into the cable. So from measuring the changes of the Hall voltage, the spent power of the driving motor can be easily obtained during the grinding process.

2.3. Response surface method

The response surface analysis is one of various methods for optimizing and evaluating the process parameters to achieve the desired output. In this method, the desired output can be represented as a function of the process parameters. The function that consists of the process parameters is called a response surface as shown in Fig. 2. In order to develop the response surface model, firstly the function must be assumed as a mathematical polynomial form having coefficients that should be determined. And then these coefficients are determined with applying the set of the experimental results.

In the case of the situation that the response surface function is related to various process parameters and a lot of experiments are conducted, the calculation for determining coefficients of the polynomial equation is very complex. And also it is difficult to finish the calculation by determining adequate coefficients that have to satisfy all

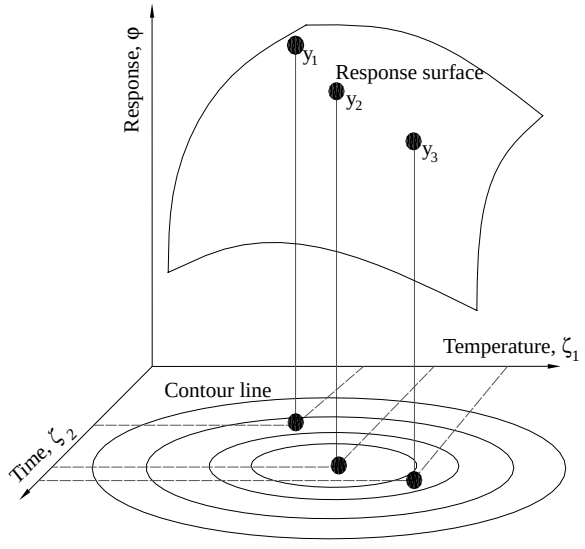

Fig. 2. Describing the concept of a response surface model.

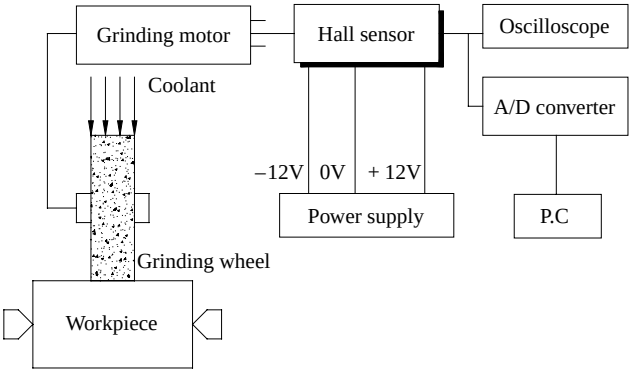

Fig. 3. Schematic drawing of used experimental set-up.

of the experimental results. The scheme of a least square error, therefore, is usually adopted and a commercial code is used for convenience of the multiple calculation.

3. Grinding experiment and obtained results

3.1. Experimental set-up

The experimental set-up for the external cylindrical grinding used in this study is shown in Fig. 3. The workpiece material was the chromium–molybdenum steel (SCM440) and heat-treated to R_c 60. This material is commonly used for rotating shafts. The grinding wheel was a type of WA120 Km V that is widely used in various industrial areas. The diameter of the wheel was 320 mm and the width 38 mm.

To evaluate the change of the grinding energy according to the various grinding conditions, three Hall effect sensors were installed in the electric cables of the grinding spindle motor. The current source of 12 V in the Hall effect sensors was supplied from a DC power supply unit. The sensitivity between the current change in the spindle motor and the output voltage in the Hall effect sensor was 0.4 V/A. The response time of the sensor was about 0.5 μs. The output voltage of the sensor was continuously measured by using an A/D converter and an oscilloscope during the grinding process. After the grinding, the surface roughness in the traverse direction in the workpiece was measured.

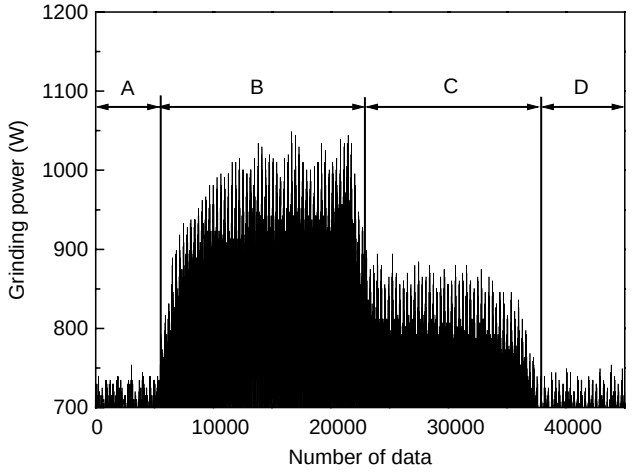

Fig. 4. Typical signal form of measured grinding power using Hall effect sensor.

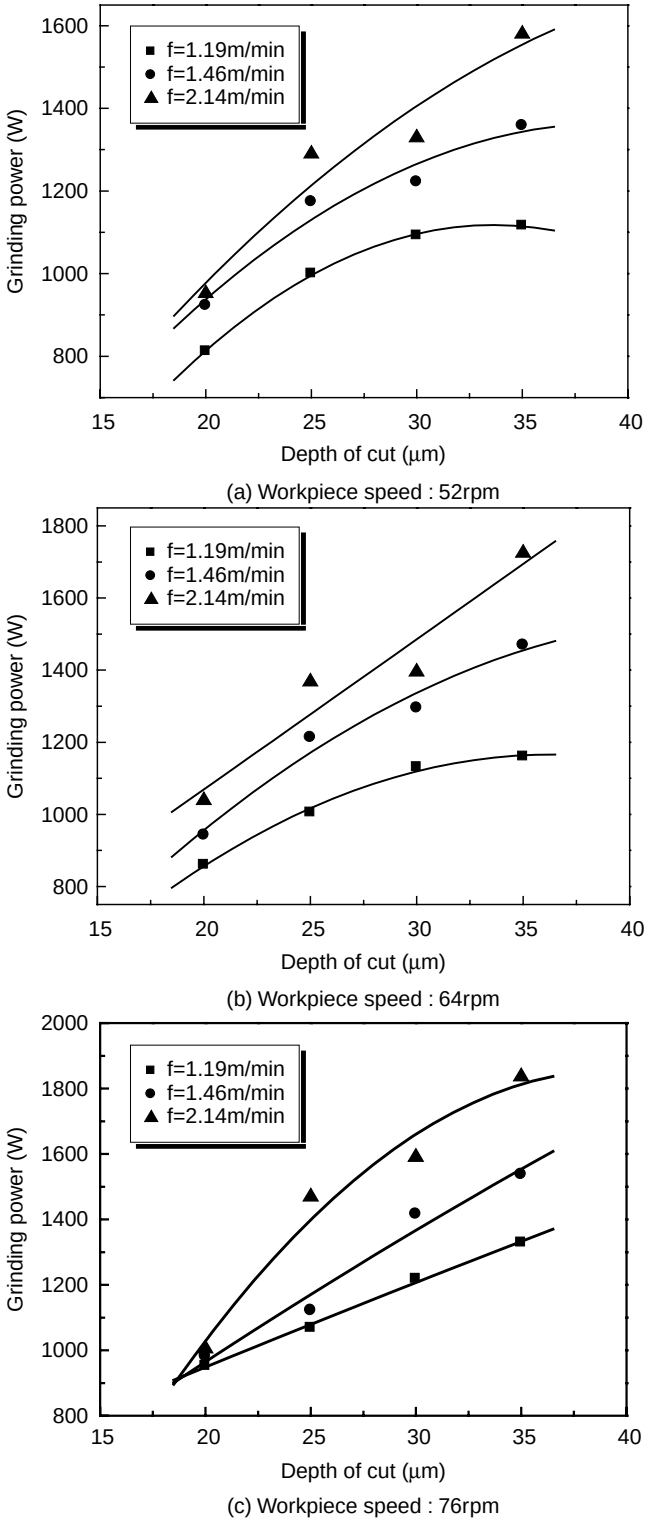

Fig. 5. Effect of depth of cut on grinding power.

In the grinding conditions, the workpiece revolution speeds were 52, 64 and 76 rpm. The depths of cut in a pass were 20, 25, 30 and 35 μm and the traverse speeds were 1. 19, 1.46 and 2.14 m/min. The wheel speed (1800 rpm) was maintained and a water-miscible coolant was supplied in all grinding experiments.

3.2. Effect of grinding conditions on power

The grinding power that was spent during the grinding process was obtained by multiplying the measured current flowing into the spindle motor cable and the supplied voltage of the motor. Fig. 4 shows a typical signal form of the grinding power during the process cycle that consisted of 4 individual parts illustrated as A, B, C and D. Region A was an idle stage with no contact between the grinding wheel and the workpiece. Although there was no contact, power was used in turning the grinding wheel. On contact between the wheel and the workpiece, the grinding power (see region B shown in Fig. 4) changed. The amount of change depended on the grinding conditions. For convenience, in this study, the total grinding power, which added the driving power to the net grinding power, was defined as

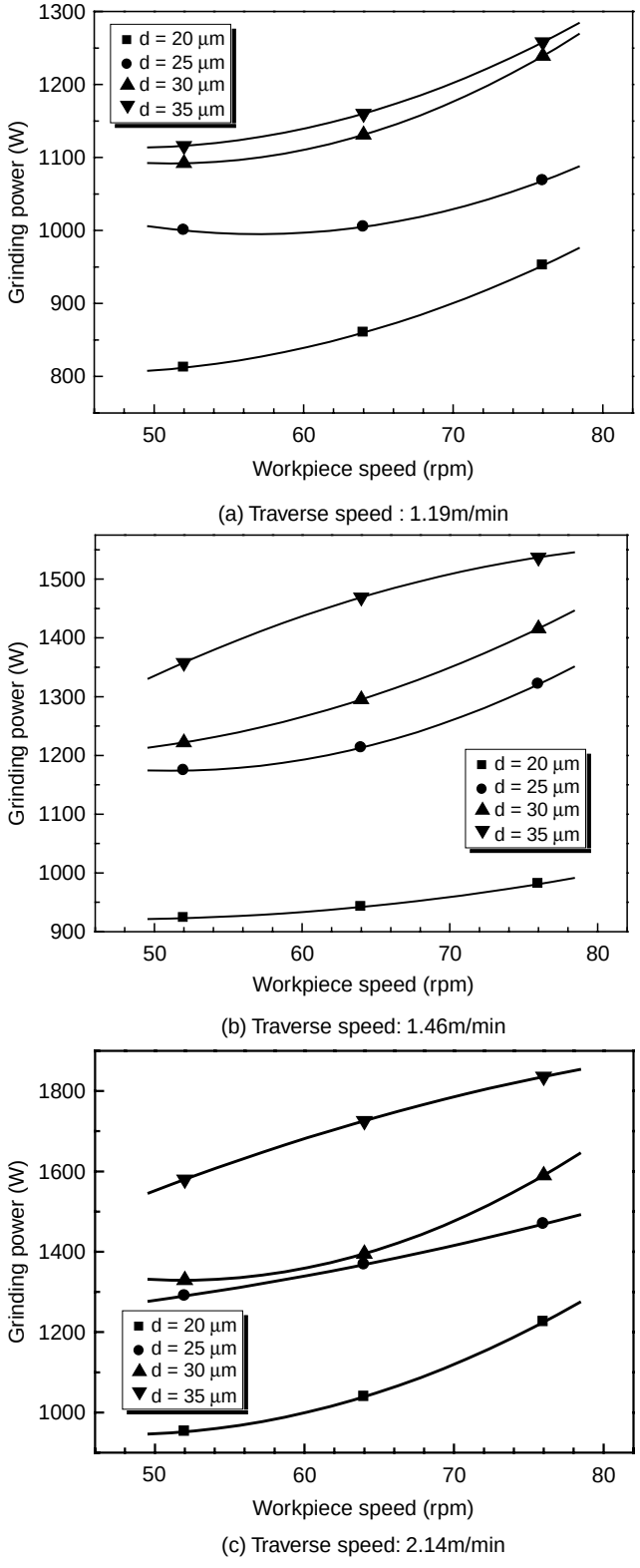

Fig. 6. Effect of workpiece speed on grinding power.

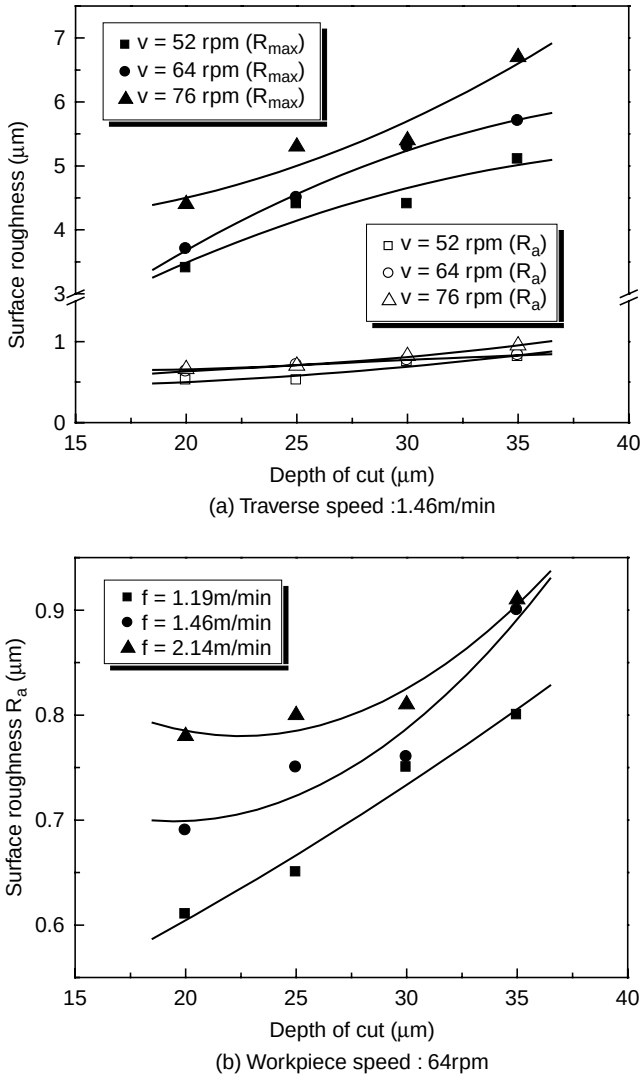

Fig. 7. Effect of depth of cut on surface roughness.

the grinding power spent during the external cylindrical grinding process. At the end of a feed forward action in the grinding wheel, the grinding wheel started the feed backward traverse, referred to spark-out motion shown in region C. As seen in region C, the grinding power was less than that of the feed forward traverse but was more than the driving power. Finally in region D, the grinding wheel disengaged the workpiece and finished the process cycle.

Fig. 5 presents the effect of the depth of cut on the grinding power for different workpiece revolution speed and traverse speed. The grinding power spent during the grinding process increased with increasing depth of cut (Fig. 6). Although the slopes of the grinding power increases were somewhat different, grinding power was also increased with increasing workpiece speed and traverse speed. The effect of the workpiece speed on grinding power is shown in Fig. 7. Although the same workpiece speed was applied, the grinding power differed about 1.6 times according to the depth of cut. From the results, it is seen that increasing the depth of cut affected the grinding power more than increasing the traverse speed.

3.3. Effect of grinding conditions on surface roughness

Fig. 7 shows the effect of depth of cut on surface roughness of the workpiece, which is measured along the traverse direction. Fig. 7 (a) shows surface roughness for different depths of cut and workpiece speeds. According to the change of the depth of cut, the maximum height (R_{max}) of the surface roughness increased proportionally but the centerline average height (R_a) changed little especially in the case of the traverse speed of 1.46 m/min. Fig. 7 (b) shows the centerline average height of the surface roughness for different depths of cut and traverse speeds.

3.4. Effect of spark-out on grinding power and surface roughness

To determine how spark-out motion affected the grinding power and the surface roughness, the experiments were conducted. The effect of the spark-out on the grinding power and the surface roughness are presented in Fig. 8.

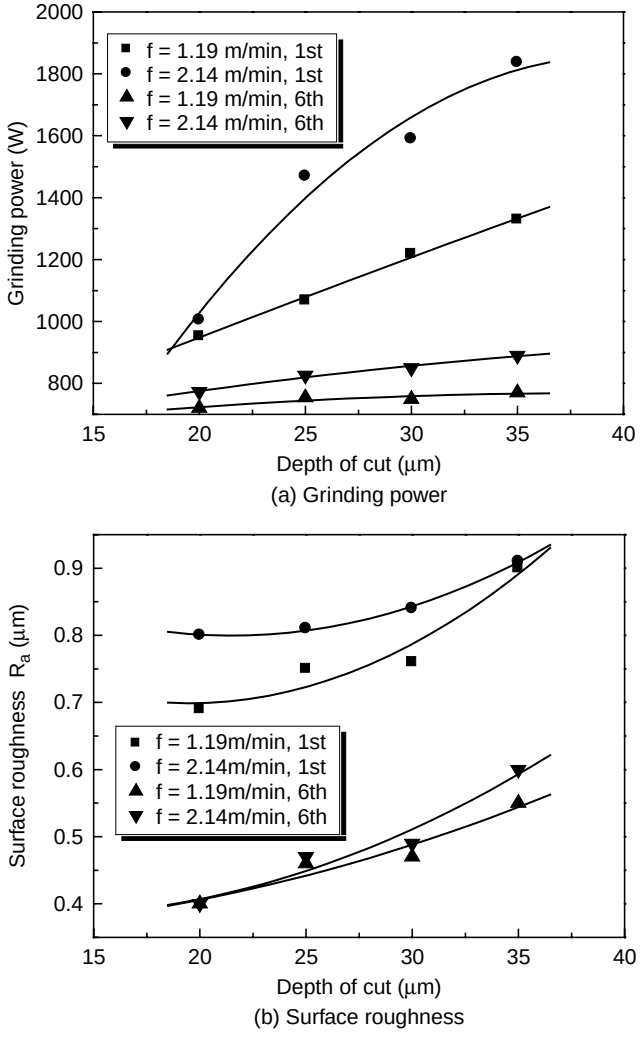

Fig. 8. Effect of spark-out on grinding power and surface roughness.

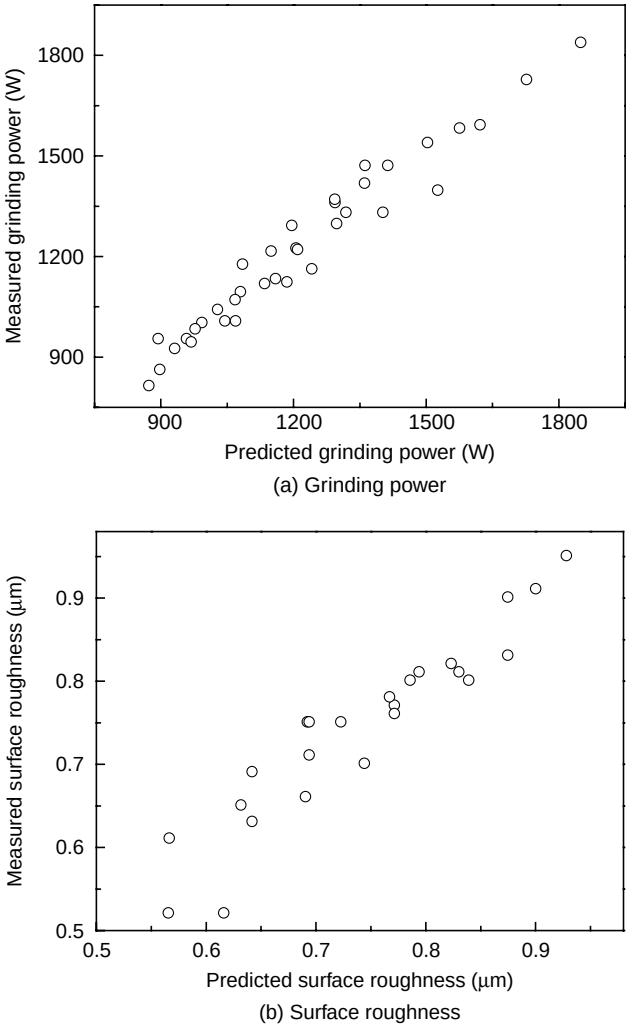

Fig. 9. Comparison between measured value and predicted value by applying developed response surface model.

In the case of the first spark-out implementation, the grinding power maintained a higher magnitude according to the depth of cut as shown in Fig. 8 (a). But in the case of the 6th spark-out implementation, the grinding power went down to near the driving power of the spindle motor at the idle stage and wasn't affected by the depth of cut or the traverse speed. In this stage, there is no more material removal. So, it was seen that material removal in external cylindrical grinding was completed after several spark-outs.

The centerline average height of the surface roughness is shown in Fig. 8 (b). After the 6th spark-out implementation, the surface roughness according to the depth of cut had not converged to a constant magnitude and a desired surface roughness in certain cases was not achieved even by several spark-outs. This is a dilemma to be solved, because more spark-outs decrease production rate but produce a good surface roughness. Therefore it is necessary to deal with this matter carefully, especially in the selection of the grinding conditions.

4. Applying response surface method

4.1. Development of response surface models

As mentioned in the previous section of this study, it is desirable to be able to forecast grinding power and surface roughness according to the grinding conditions. One means of doing this is to represent grinding outcomes mathematically as a function of the applicable grinding parameters. In this study, the response surface method was used to achieve the aim. Second-order response surface models using the workpiece revolution speed v (rpm), the traverse speed f (m/min) and the depth of cut d (μm) were developed as

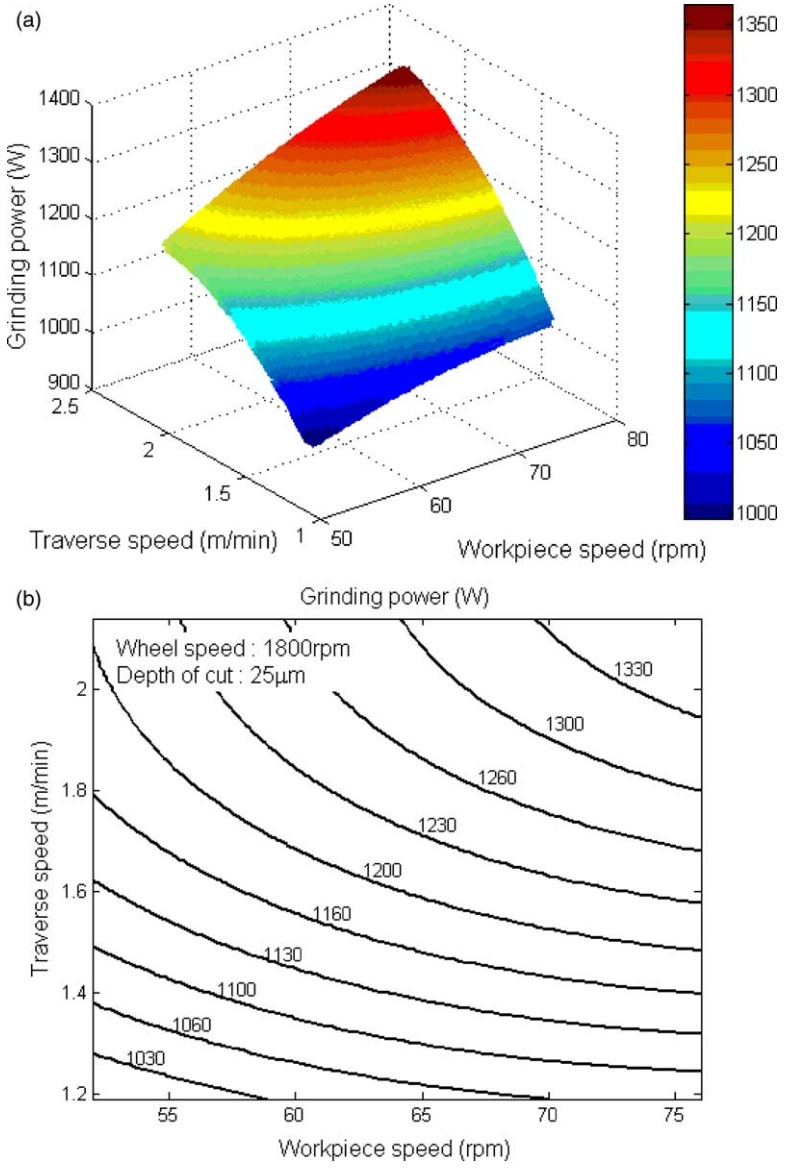

Fig. 10. Response surface and contour plot of grinding power according to change of workpiece speed and traverse speed.

below.

$$P_o = 359.83797 - 0.10070v^2 - 184.65033f^2 - 0.65000d^2 + 3.95418vf + 0.45254vd + 24.94593fd \quad (4)$$

$$R_a = 0.21369 - 0.00009v^2 - 0.09995f^2 + 0.00051d^2 + 0.01156vf + 0.00002vd - 0.00979fd \quad (5)$$

Where, the symbol P_o (W) was the grinding power and R_a (μm) the surface roughness. Fig. 9 shows the difference between the measured quantity and the predicted quantity by applying the developed response surface models lists in Eqs. (4) and (5). As shown in Fig. 9(a), the predicted grinding power well coincides with the measured grinding power and also the predicted surface roughness shown in Fig. 9(b) corresponded with the measured value although it had some wide deviation in the distribution.

Fig. 10 presents an example of the response surface and contour plots of the grinding power according to the change of the workpiece speed and the traverse speed. In these plots, the depth of cut was fixed as 25 μm. The 3D plot of

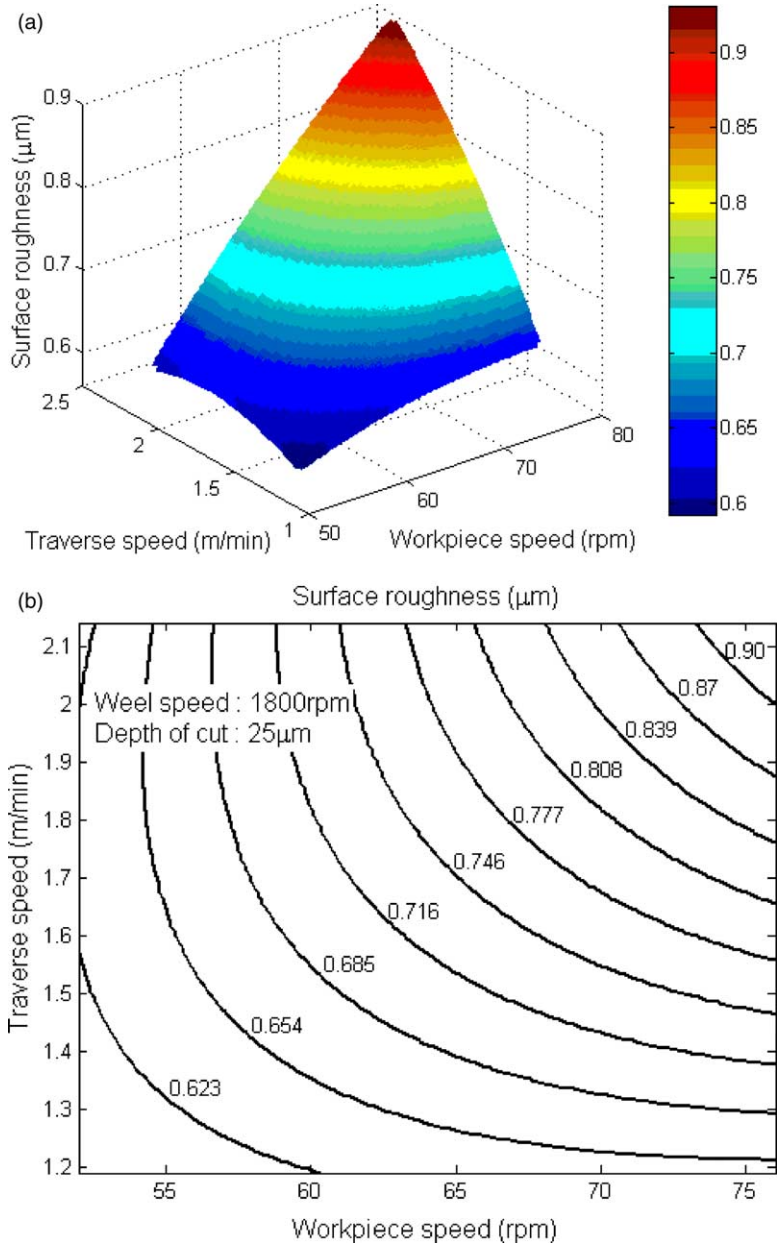

Fig. 11. Response surface and contour plot of surface roughness according to change of workpiece speed and traverse speed.

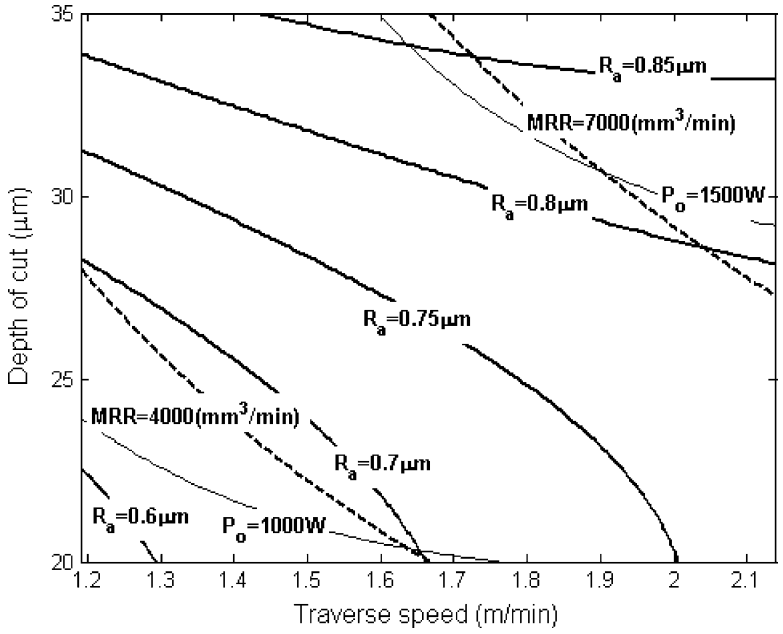

Fig. 12. Contour plot of surface roughness with constraints of material removal rate and grinding power for selecting permissible range of grinding conditions.

the grinding power shown in Fig. 10 (a) seems to increase linearly in accordance with increasing the workpiece speed and the traverse speed. But from the contour plot shown in Fig. 10 (b), it is seen that the traverse speed has a greater influence on the grinding power. A small change of the traverse speed with a fixed workpiece speed, affected the grinding power.

The 3D plot of the surface roughness, as represented in Fig. 11, shows a more rapid change than the grinding power according to the workpiece speed and the traverse speed. The surface roughness was dominantly affected by the change of the workpiece speed.

4.2. Validation of developed response surface models

In past decades, selecting the grinding conditions strongly depended upon an expert's judgment. So, it was very difficult for beginners or unskilled workers to determine the proper grinding conditions to satisfy all demanded constraints such as the surface roughness, the material removal rate and the grinding power to be spent. The developed response surface models enable selection of the grinding conditions without much grinding experience. The material removal rate per minute, MRR (mm^3/min), during the external cylindrical grinding can be written as follows:

$$\mathrm{MRR}(\mathrm{mm}^3/\mathrm{min}) = d * f * D_\mathrm{a} \tag{6}$$

In Eq. (6), the symbol D_a (mm) represents the average diameter of the used workpiece. If three constraints for industrial application were as Eqs. (7)–(9), the selected grinding conditions have to satisfy all constraints. Although it looks like a conventional optimization problem, it can be simply solved by using the developed response surface models.

$$0.70 \le R_\mathrm{a}(\mu\mathrm{m}) \le 0.85 \tag{7}$$

$$4000 \le \mathrm{MRR}(\mathrm{mm}^3/\mathrm{min}) \le 7000 \tag{8}$$

$$1000 \le P_\mathrm{o}(W) \le 1500 \tag{9}$$

An example is presented in Fig. 12. In this case, the workpiece revolution speed was fixed as 64 rpm. Firstly the contour plot of the surface roughness was drawn according to the change of the traverse speed and the depth of cut and then the given constraint ranges at the material removal rate and the grinding power were added into the contour plot. Now, the grinding conditions satisfying all constraints can be determined by selecting an inside region enclosed by the constraints' lines.

5. Concluding remarks

In this study, the response surface method was applied for analyzing the grinding power and the surface roughness in the external cylindrical grinding of the hardened SCM440 material. A Hall effect sensor was used to measure the grinding power of the spindle driving motor during the grinding.

Based on experimental results, increasing the depth of cut affected the grinding power more than increasing

the traverse speed. In addition, increasing the depth of cut changed the maximum height of the surface roughness more than the centerline average height. After several spark-outs, the grinding power went down to near the driving power but, in certain cases, the desired surface roughness was not obtained.

By using the grinding parameters, the second-order response surface models for the grinding power and the surface roughness in the external cylindrical grinding were developed. Therefore, it is possible to predict the grinding power and the surface roughness before conducting grinding, and the grinding conditions satisfying constraints for industrial application can be selected very easily from the contour plot of the developed response surface models.

References

[1] E.S. Lee, N.H. Kim, A study on the machining characteristics in the experimental plunge grinding using the current signal of the spindle motor, International Journal of Machine Tools & Manufacture 41 (7) (2001) 937–951.

[2] Z.B. Hou, R. Komanduri, On the mechanics of the grinding process, part 2-thermal analysis of fine grinding, International Journal of Machine Tools & Manufacture 44 (2–3) (2004) 247–270.

[3] T. Kuriyagawa, K. Syoji, H. Ahshita, Grinding temperature within contact arc between wheel and workpiece in high-efficiency grinding of ultrahard cutting tool materials, Journal of Materials Processing Technology 136 (1–3) (2003) 39–47.

[4] A.V. Gopal, P.V. Rao, Selection of optimum conditions for maximum material removal rate with surface finish and damage as constraints in SiC grinding, International Journal of Machine Tools & Manufacture 43 (1–3) (2003) 1327–1336.

[5] B. Lin, S.Y. Yu, S.X. Wang, An experimental study on molecular dynamics simulation in nanometer grinding, Journal of Materials Processing Technology 138 (1–3) (2003) 484–488.

[6] M.N. Dhavlikar, M.S. Kulkarni, V. Mariappan, Combined Taguchi and dual response method for optimization of a centerless grinding operation, Journal of Materials Processing Technology 132 (1–3) (2003) 90–94.

[7] X. Xu, Y. Yu, H. Huang, Mechanisms of abrasive wear in the grinding of titanium (TC4) and nickel (K417) alloys, Wear 255 (7–12) (2003) 1421–1426.

[8] S. Malkin, Grinding Technology-theory and Applications of Machining with Abrasives, Wiley, New York, 1989.

[9] T.W. Hwang, S. Malkin, Upper bound analysis for specific energy in grinding of ceramics, Wear 231 (2) (1999) 161–171.

[10] S. Shaji, V. Radhakrishnan, Analysis of process parameters in surface grinding with graphite as lubricant based of the Taguchi method, Journal of Materials Processing Technology 141 (1) (2003) 51–59.

[11] J-S Kwak, Application of Taguchi and response surface methodologies for geometric error in surface grinding process, International Journal of Machine Tools and Manufacture 45 (3) (2005) 327–334.